THE ASTROPHYSICAL JOURNAL, 527:L81–L84, 1999 December 20

THE MASS FUNCTION OF YOUNG STAR CLUSTERS IN THE "ANTENNAE" GALAXIES

QING ZHANG[1,2] AND S. MICHAEL FALL[1]

Received 1999 September 27; accepted 1999 October 19; published 1999 November 22

ABSTRACT

We determine the mass function of young star clusters in the merging galaxies known as the "Antennae" (NGC 4038/9) from deep images taken with the Wide Field Planetary Camera 2 on the refurbished *Hubble Space Telescope*. This is accomplished by means of reddening-free parameters and a comparison with stellar population synthesis tracks to estimate the intrinsic luminosity and age, and hence the mass, of each cluster. We find that the mass function of the young star clusters (with ages $\lesssim$160 Myr) is well represented by a power law of the form $\psi(M) \propto M^{-2}$ over the range $10^4 \lesssim M \lesssim 10^6\ M_\odot$. This result may have important implications for our understanding of the origin of globular clusters during the early phases of galactic evolution.

Subject headings: galaxies: individual (NGC 4038/9) — galaxies: interactions — galaxies: star clusters

1. INTRODUCTION

The luminosity functions of the young star clusters in merging galaxies, including the "Antennae" (NGC 4038/9), have roughly power-law form, $\phi(L) \propto L^\alpha$ with $\alpha \approx -2$, and no sign of a peak or turnover down to the limiting magnitudes of the observations (Whitmore & Schweizer 1995; Schweizer et al. 1996; Miller et al. 1997; Carlson et al. 1998; Whitmore et al. 1999; Zepf et al. 1999). These are similar to the luminosity functions of open clusters in the Milky Way (van den Bergh & LaFontaine 1984) and M33 (Christian & Schommer 1988) and of the populous clusters in the LMC (Elson & Fall 1985) and starburst galaxies (Meurer et al. 1995). In contrast, the luminosity functions of the old globular clusters in the Milky Way, the Andromeda galaxy, and elliptical galaxies have peaks at $L_V \approx 10^5\ L_\odot$ and decline toward both higher and lower luminosities. These functions are often represented by lognormal distributions of luminosities, corresponding to Gaussian distributions of magnitudes (e.g., Harris 1991).

This immediately raises the question of whether the mass functions of the young star clusters in merging galaxies have power-law or lognormal forms. The mass functions are of greater relevance to our understanding of the physical processes involved in the formation and disruption of the clusters. If the star clusters of any population formed at the same time and with the same stellar initial mass function (IMF), then the luminosity function of the clusters would always have the same shape as the mass function, the two being related by a time-dependent shift along the luminosity axis. However, if the spread in ages within a population is comparable to the mean age, as seems likely for the young star clusters in some recent mergers, one might then worry about the effects of fading, which could cause the shape of the luminosity function to differ substantially from the shape of the mass function (Hogg & Phinney 1997). Based on simulations of this effect, Meurer (1995) concluded that the power-law luminosity function in the Antennae, derived by Whitmore & Schweizer (1995) from observations with the Wide Field Planetary Camera 1 (WFPC1) before the refurbishment of the *Hubble Space Telescope* (*HST*), may be consistent with an underlying lognormal mass function. Furthermore, Fritze–von Alvensleben (1999) estimated the mass function of young star clusters in the Antennae directly from these WFPC1 observations and found a lognormal form similar to that of old globular clusters.

The purpose of this Letter is to determine the mass function of the young star clusters in the Antennae from images taken with the WFPC2 after the refurbishment of *HST*; these extend about 2 mag fainter than the earlier images taken with the WFPC1. The data reduction and luminosity functions are described in detail by Whitmore et al. (1999). The novelty of our approach for determining the mass function is that we use reddening-free parameters and a comparison with stellar population synthesis tracks to estimate the intrinsic luminosity and age, and hence the mass, of each cluster.

2. OBSERVATIONS AND SELECTION OF CLUSTERS

The Antennae galaxies were observed with the WFPC2 in 1996 January for 2000–4500 s with each of the broadband filters F336W, F439W, F555W, and F814W. Pointlike objects were identified and their magnitudes measured with the IRAF task DAOPHOT; photometry in this system was then transformed to the Johnson *UBVI* system. About 11,000 objects were detected with $17.4 < V < 25.4$, corresponding to $-14 < M_V < -6$ at the adopted distance of 19.2 Mpc (for H_0 = 75 km s^{-1} Mpc^{-1}). Much of our analysis is based on the reddening-free parameters

$$Q_1 = (U - B) - 0.72\,(B - V), \tag{1}$$

$$Q_2 = (B - V) - 0.80\,(V - I). \tag{2}$$

The first of these is the standard reddening-free parameter in the *UBV* system, while the second is a direct extension to the *UBVI* system. Other reddening-free parameters can be defined analogously, but they are all linear combinations of Q_1 and Q_2. Equations (1) and (2) are based on the Galactic extinction curve but would be virtually the same for other familiar extinction curves, such as those of the Magellanic Clouds. For objects with $M_V = -9$, the photometric errors in *U*, *B*, *V*, and *I* (0.04–0.07) lead to 1 σ uncertainties of 0.12 in Q_1 and 0.11 in Q_2.

We identify cluster candidates and estimate their extinctions and ages by comparing them with population synthesis tracks in the Q_1Q_2 diagram, shown here as Figure 1. In the presence of reddening by dust, this approach has significant advantages over methods based on the more familiar two-color diagrams.

[1] Space Telescope Science Institute, 3700 San Martin Drive, Baltimore, MD 21218; qzhang@stsci.edu, fall@stsci.edu.

[2] Henry A. Rowland Department of Physics and Astronomy, Johns Hopkins University, 3400 North Charles Street, Baltimore, MD 21218.

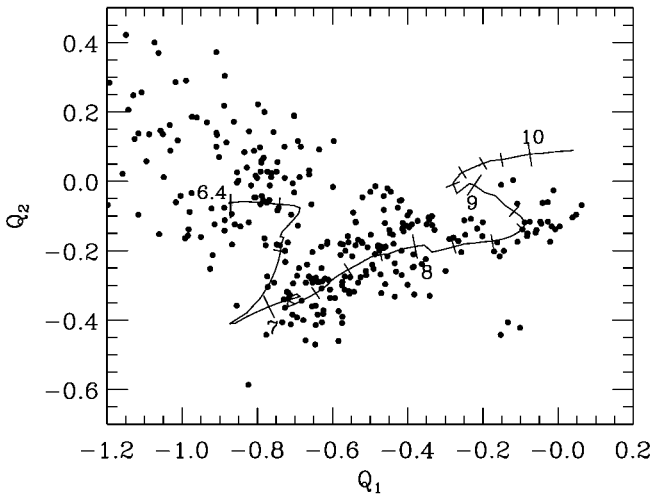

FIG. 1.—Q_1Q_2 diagram. The line represents the BC96 population synthesis track with the indicated values of log (t/yr) and tick marks every $\Delta \log t$ = 0.2. In this model, the Q-parameters remain constant for log (t/yr) < 6.4. The dots are all the cluster candidates in our sample with estimated masses above $10^5\ M_\odot$.

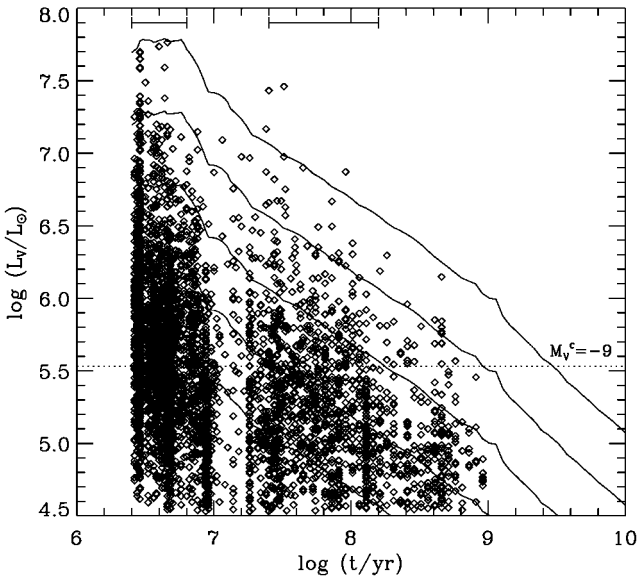

FIG. 2.—Extinction-corrected luminosities of cluster candidates as a function of their ages. The lines represent the BC96 population synthesis tracks with log ($M/M_\odot$) = 6.0, 5.5, 5.0, 4.5, and 4.0. The bars at the top indicate the intervals of age adopted to determine the mass function. The horizontal dotted line at $M_V^c = -9$ (extinction-corrected) indicates the upper limit of stellar contamination.

For the population synthesis track, we use the G. Bruzual & S. Charlot (1996, unpublished, hereafter BC96) model with the Salpeter IMF truncated at 0.1 and 125 $M_\odot$ and with solar metallicity. We regard all pointlike objects brighter than $M_V = -9$ as cluster candidates, irrespective of their Q-parameters, because nearly all known stars are fainter than this limit (Humphreys 1983). Furthermore, we regard fainter pointlike objects as cluster candidates if they lie within $\Delta Q = (\Delta Q_1^2 + \Delta Q_2^2)^{1/2} = 0.3$ of the population synthesis track (except for a few objects with extremely large photometric errors). This procedure eliminates some but not all stars from our sample (see Figs. 13 and 14 of Whitmore et al. 1999). However, as shown below, stellar contamination has little effect on the mass function that we derive because this is based mainly on the brightest objects.

For each cluster candidate, we estimate the intrinsic colors, age t, and mass-to-light ratio M/L from the nearest point on the population synthesis track in the Q_1Q_2 diagram. A comparison of the intrinsic with the observed colors gives the extinction A_V, and the intrinsic luminosity L_V and mass M then follow from V and A_V. The mean value of A_V varies from 1.5 for the youngest clusters ($t < 10$ Myr) to 0.3 for the oldest clusters ($t > 100$ Myr). Because the BC96 population synthesis track stops evolving in the Q_1Q_2 diagram at log (t/yr) = 6.4, no objects can be assigned ages smaller than this by our procedure. Instead, the youngest clusters are all assigned ages in the interval $6.4 < \log (t/\mathrm{yr}) < 6.8$. Furthermore, because the track bends sharply at log (t/yr) ≈ 6.9 and has a zigzag at log (t/yr) ≈ 7.2, there is some ambiguity in the assignment of ages in this region of the Q_1Q_2 diagram. For these reasons, we exclude the intervals $\log (t/\mathrm{yr}) < 6.4$ and $6.8 < \log (t/\mathrm{yr}) < 7.4$ from our determination of the mass function.

We have verified by simulations that the scatter of cluster candidates away from the population synthesis track in the Q_1Q_2 diagram is mostly accounted for by photometric errors. However, for the youngest objects ($t < 10$ Myr), the scatter is slightly larger, probably because they are affected by nebular emission and residual extinction. (While or method is designed to correct for extinction, this is not always perfect, especially in the dusty regions where the youngest clusters are often found.) The errors in the Q-parameters lead to typical uncertainties of a factor of 2 in the ages and factors that vary from 1.1 to 1.7 in the luminosities. Fortunately, these uncertainties tend to cancel out in estimates of the masses, because younger clusters have lower mass-to-light ratios but higher extinctions. As a result, the uncertainties in the masses of most cluster candidates are better than 50%.

Figure 2 shows the luminosity-age relation for the objects in our sample along with the BC96 population synthesis tracks for log ($M/M_\odot$) = 6.0, 5.5, 5.0, 4.5, and 4.0. Evidently, the masses of the cluster candidates range from well below $10^4\ M_\odot$ to just above $10^6\ M_\odot$. The apparent gaps in the luminosity-age relation at log (t/yr) < 6.4 and 7.0 < log (t/yr) < 7.2 are artifacts caused by little or no evolution of the population synthesis track in the Q_1Q_2 diagram in these intervals of age (discussed above). Stellar contamination can be neglected above the horizontal dotted line in Figure 2 at $M_V^c = -9$, an extinction-corrected magnitude that excludes all but the very brightest stars. For reference, the Large Magellanic Cloud, with about 4% of the total blue luminosity of the Antennae, has two stars with $M_V^c = -9$, three with $-10 < M_V^c < -9$, and none with $M_V^c < -10$ (Humphreys 1983). Thus, we might expect ~100 stars (mostly blue supergiants) brighter than $M_V^c = -9$ in our sample of cluster candidates, i.e., contamination at just the ~5% level.

3. MASS FUNCTION OF CLUSTERS

We construct the mass function of cluster candidates in two intervals of age: $6.4 < \log (t/\mathrm{yr}) < 6.8$ and $7.4 < \log (t/\mathrm{yr}) < 8.2$, corresponding to $2.5 < t < 6.3$ Myr and $25 < t < 160$ Myr. These intervals, which are indicated by the bars at the top of Figure 2, were chosen to avoid the problems discussed in the previous section. The first allows us to estimate the mass function down to relatively low masses with a relatively large num-

ber of objects, while the second provides a check on the consistency of our procedure. In constructing the mass function, we must correct for incompleteness in our sample. This depends on the brightness of the objects, whether they are on the PC or WF chips, and the local background and/or crowding. For each cluster candidate, we adopt the completeness factor determined by Whitmore et al. (1999) using a false-star method. Our sample as a whole is about 50% complete at $V = 24$, corresponding to $\log (M/M_\odot) \approx 3.9$ for $6.4 < \log (t/\mathrm{yr}) < 6.8$ and $\log (M/M_\odot) \approx 4.4$ for $7.4 < \log (t/\mathrm{yr}) < 8.2$. Above these limits, the younger and older subsamples contain 1140 and 477 objects, respectively.

Figure 3 shows the completeness-corrected mass functions of the cluster candidates in the two intervals of age. The stellar contamination limits are labeled "S," while the completeness limits are labeled "C." Stellar contamination is negligible for the younger subsample, but it could begin to affect the older subsample for $\log (M/M_\odot) \lesssim 4.7$. Evidently, the mass functions for the two subsamples are nearly indistinguishable above the completeness limits. They can be represented by a power law, $\psi(M) \propto M^\beta$, with $\beta = -1.95 \pm 0.03$ for $6.4 < \log (t/\mathrm{yr}) < 6.8$ and $\beta = -2.00 \pm 0.08$ for $7.4 < \log (t/\mathrm{yr}) < 8.2$. These are based on weighted least-square fits of the form $\log \psi = \beta \log M + \mathrm{const}$.

We have checked that our results are robust with respect to the adopted population synthesis tracks. First, we repeated the entire analysis with the BC96 models but with a different IMF (Scalo vs. Salpeter) and different metallicities (0.4 and 2.5 $Z_\odot$ vs. 1.0 $Z_\odot$). Second, we repeated the analysis with the Leitherer et al. (1999) models with the Salpeter IMF and solar metallicity. In the first case, the mass function was virtually the same; in the second case, it was slightly steeper, with $\beta = -2.1$. We have also checked that our results are not biased by observational errors by randomly reassigning ages to all cluster candidates younger than $\log (t/\mathrm{yr}) = 6.8$. In this case, we obtain $\beta = -1.9$.

Figure 3 shows a comparison between the mass function of the young star clusters in the Antennae determined here and the mass function of old globular clusters (indicated by the dashed curves). The latter was derived from the usual Gaussian distribution of magnitudes and a fixed mass-to-light ratio, $M/L_V = 2$. Within the observational uncertainties, it appears that the two mass functions may be similar for $M \gtrsim 2 \times 10^5\ M_\odot$. However, for $M \lesssim 2 \times 10^5\ M_\odot$, they are completely different; that for the young clusters in the Antennae increases rapidly, while that for the old globular clusters decreases rapidly. Whitmore et al. (1999) found that the luminosity function of the star clusters in the Antennae could be described by two power laws joined by a weak bend (with $\alpha_1 = -1.7$ and $\alpha_2 = -2.6$), and there may also be hints of curvature in the mass function that we have derived. However, any such deviations in the latter from a single power law have low statistical significance ($<2\ \sigma$). Alternatively, the bend in the luminosity function may result from the fading of clusters that formed over a period of a few hundred megayears with a power-law mass function truncated near $10^6\ M_\odot$.

Our results differ substantially from those based on earlier observations of the Antennae with the WFPC1 on *HST* (Meurer 1995; Fritze–von Alvensleben 1999). To understand this difference, we have performed two tests. First, we artificially truncated our sample at $M_V = -9.6$, the same limit adopted by Fritze–von Alvensleben, and then repeated the entire analysis described above. (Note that after corrections for extinction,

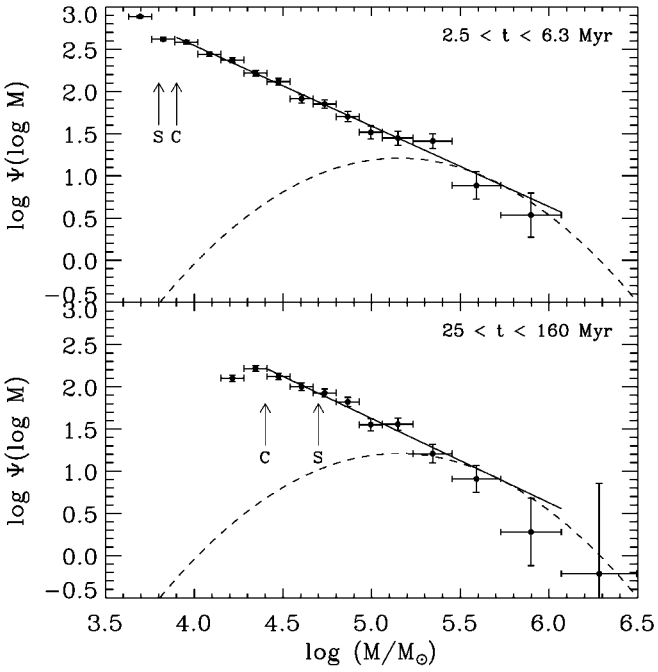

FIG. 3.—Completeness-corrected mass function $\Psi(\log M) = M\psi(M)$ of cluster candidates in two intervals of age: $6.4 < \log (t/\mathrm{yr}) < 6.8$ (*top*) and $7.4 < \log (t/\mathrm{yr}) < 8.2$ (*bottom*). The vertical and horizontal bars indicate the 1 σ Poisson uncertainties and the bin sizes, respectively. The arrows labeled S indicate the stellar contamination limit ($M_V^c \approx -9$), and the arrows labeled C indicate the 50% completeness limit ($V \approx 24$). The solid lines are power laws, $\psi(M) \propto M^\beta$, with $\beta = -1.95 \pm 0.03$ and $\beta = -2.00 \pm 0.08$, respectively, for the younger and older clusters. The dashed line represents a lognormal mass function, derived from a Gaussian distribution of magnitudes with a mean $\langle M_V \rangle = -7.3$ and dispersion $\sigma(M_V) = 1.2$ (Harris 1991) and a fixed mass-to-light ratio of $M/L_V = 2$.

$M_V = -9.6$ corresponds approximately to $M_V^c = -9.9$ to -11.1). In this case, we obtained a mass function similar to the lognormal one found by Fritze–von Alvensleben. Second, we performed a simulation in which clusters were drawn from a power-law mass function (with $\beta = -2$) and a uniform age distribution. The luminosities of the clusters were then computed from the BC96 population synthesis models. For simulated clusters brighter than $M_V = -9.6$, the mass function again resembled the one found by Fritze–von Alvensleben. The reason for this is that, because the clusters fade, those with high masses can be observed over a wide range of ages, whereas those with low masses can be observed only when they are young. As a result, low-mass clusters are underrepresented in the observed mass function, which therefore declines toward both high and low masses.

4. DISCUSSION

We have found that the mass function of young star clusters in the Antennae is well represented by a power law, $\psi(M) \propto M^{-2}$, over the range $10^4 \lesssim M \lesssim 10^6\ M_\odot$. This is similar to the power-law mass function of diffuse and molecular clouds in the Milky Way (Dickey & Garwood 1989; Solomon & Rivolo 1989). However, it differs radically from the lognormal mass function of old globular clusters, which peaks at a few times $10^5\ M_\odot$ and declines rapidly toward both higher and lower masses. It is widely believed that galaxies formed hierarchically by the merging of smaller galaxies and/or subgalactic frag-

ments. Thus, our results have potentially important implications concerning the origin of globular clusters during the early phases of galactic evolution. In this connection, it is worth emphasizing that a power-law mass function is "scale free," whereas a lognormal mass function has a "preferred scale."

One explanation for the different mass functions is that the conditions in ancient galaxies and protogalaxies were such as to imprint a characteristic mass of a few times $10^5\ M_\odot$ but that these conditions no longer prevail in modern galaxies. For example, the minimum mass of newly formed star clusters, set by the Jeans mass of interstellar clouds, will be high when the gas cannot cool efficiently and low when it can, which in turn will depend on the abundances of heavy elements and molecules, the strength of any heat sources, and so forth. These effects favor the formation of clusters in a narrower range of masses in the past than at present (Fall & Rees 1985; Kang et al. 1990). Another explanation for the different mass functions is that populations of star clusters were born scale free but later acquired a preferred scale by the selective disruption of low-mass clusters (Fall & Rees 1977; Gnedin & Ostriker 1997 and references therein). In this case, a power-law mass function might evolve into a lognormal mass function (Okazaki & Tosa 1995; Elmegreen & Efremov 1997; Baumgardt 1998; Vesperini 1998). We plan to address this issue in a future paper.

We thank Claus Leitherer and Brad Whitmore for valuable discussions. Support for this work was provided by NASA through grant GO-07468 from STScI.

REFERENCES

Baumgardt, H. 1998, A&A, 330, 480
Carlson, M. N., et al. 1998, AJ, 115, 1778
Christian, C. A., & Schommer, R. A. 1988, AJ, 95, 704
Dickey, J. M., & Garwood, R. W. 1989, ApJ, 341, 201
Elmegreen, B. G., & Efremov, Y. N. 1997, ApJ, 480, 235
Elson, R. A. W., & Fall, S. M. 1985, PASP, 97, 692
Fall, S. M., & Rees, M. J. 1977, MNRAS, 181, 37P
———. 1985, ApJ, 298, 18
Fritze–von Alvensleben, U. 1999, A&A, 342, L25
Gnedin, O. Y., & Ostriker, J. P. 1997, ApJ, 474, 223
Harris, W. E. 1991, ARA&A, 29, 543
Hogg, D. W., & Phinney, E. S. 1997, ApJ, 488, L95
Humphreys, R. M. 1983, ApJ, 269, 335
Kang, H., Shapiro, P. R., Fall, S. M., & Rees, M. J. 1990, ApJ, 363, 488
Leitherer, C., et al. 1999, ApJS, 123, 3
Meurer, G. R. 1995, Nature, 375, 742
Meurer, G. R., Heckman, T. M., Leitherer, C., Kinney, A., Robert, C., & Garnett, D. R. 1995, AJ, 110, 2665
Miller, B. W., Whitmore, B. C., Schweizer, F., & Fall, S. M. 1997, AJ, 114, 2381
Okazaki, T., & Tosa, M. 1995, MNRAS, 274, 48
Schweizer, F., Miller, B. W., Whitmore, B. C., & Fall, S. M. 1996, AJ, 112, 1839
Solomon, P. M., & Rivolo, A. R. 1989, ApJ, 339, 919
van den Bergh, S., & LaFontaine, A. 1984, AJ, 89, 1822
Vesperini, E. 1998, MNRAS, 299, 1019
Whitmore, B. C., Miller, B. W., Schweizer, F., & Fall, S. M. 1997, AJ, 114, 1797
Whitmore, B. C., & Schweizer, F. 1995, AJ, 109, 960
Whitmore, B. C., Zhang, Q., Leitherer, C., Fall, S. M., Schweizer, F., & Miller, B. W. 1999, AJ, 118, 1551
Zepf, S. E., Ashman, K. M., English, J., Freeman, K. C., & Sharples, R. M. 1999, AJ, 118, 752